Math 142 Final Project: MCM 2021 Problem B

Lily Covarrubias, AJ Fong, Frank Hobson, Reina Schmoock, Da-Yi Wu

December 2025

Contents

1 Summary

Our problem asked us to develop a drone procurement and utilization program to tackle bushfires in Victoria, Australia. Specifically, we had to determine the optimal allocation of **Surveillance and Situation Awareness (SSA) drones** to **Radio Repeater drones**, the number of drones needed to future-proof the program, how to place the drones in an active bushfire, and provide a budget for the program to the Victoria Country Fire Authority.

Though our group addressed all aspects of the problem statement, the most effort was dedicated to the optimal placement of drones in an active bushfire. We assumed that drones all fly the same, cost the same, and their only difference is functional. For the fires, though a model for fire spread is provided, it was not used in the model to place drones. For that model, we assumed fires were all circular, and the distribution of drones focused on that space.

We find that firefighters stopped the majority of bushfires in Victoria's history before becoming major concerns, and are not the reason why drones are being considered. Accordingly, we restricted our analysis to the largest fires in Victoria's history, with burned areas exceeding 2,000 hectares. These were further sub-classified into "small fires" and "large fires," where small fires were 2,000-10,000 hectares in size and large fires exceeded 10,000 hectares in size. Based on historical fire data, we find a total of **14** drones satisfy the requirements of our small fires, and **330** drones would be needed for the largest fire in Victoria's history. We then show how the drones would be distributed across Victoria's terrain using our joint PSO-Greedy methods below.

We utilized two models to determine the optimal placement of drones: **Particle Swarm Optimization (PSO)** and **Greedy Search**. Particle Swarm Optimization was our best model for the SSA drones, and Greedy Search was used for the radio repeater drones. We applied these methods to a 2D and a 3D case to represent various bushfires. The 2D case sufficiently models drone placement for fires on flat-enough terrain, or small fires on any terrain. The 3D case is sufficient for large fires over Victoria's terrain and considers the terrain when determining drone placement.

Using data from historical fires, we present an upper bound on the number of drone charges needed for an individual bushfire event. We also demonstrate that the number of wildfires under our filter has not increased, indicating no additional drones are needed to future-proof the program. In the final section, we present the budget model that shows our drone program would require an estimated **$6,361,760**, given the expected number of small (80) and large (40) fire events over 10 years. This would cover the drones and electricity, but not the personnel and training needed to operate the drones.

We successfully answer all four aspects of the Country Fire Authority's problem statement in this report, and eagerly await its implementation for future firefighting efforts. All code used for our report can be found in our GitHub repository.

2 Introduction

In light of the repeated fires in Victoria across the 2019-20 and 2023-24 bushfire seasons, the Premier of Victoria has contracted us to help implement a drone-assisted firefighting strategy. Our job is to determine the number of Surveillance and Situational Awareness (SSA) and Radio Repeater drones needed to effectively monitor the spread of wildfires and relay the information to the Emergency Operations Center (EOC). In this paper, we will do the following:

1. Create a model to determine the optimal numbers and mix of SSA drones and Radio Repeater drones to purchase for a proposed new division, "Rapid Bushfire Response," of Victoria's Country Fire Authority (CFA). The model should balance capability and safety with economics, as well as consider observational and communications mission needs and topography. The model should also incorporate fire event size and frequency as parameters.

2. Illustrate how the model adapts to the changing likelihood of extreme fire events over the next decade. Project what equipment cost increases will occur assuming the cost of drone systems stays constant.

3. Determine a model for optimizing the locations of hovering VHF/UHF radio-repeater drones for fires of different sizes on different terrains.

4. Prepare a one- to two-page **annotated Budget Request** supported by your models for *CFA* to submit to the Victoria State Government.

Our work involves analyzing the topography of Victoria, investigating fire spread models, and designing an efficient drone coverage framework to balance safety and budget limitations. Integrating environmental modeling with strategy based drone deployment allows for the enhancement of early detection, improved communication, and informed decision making during wildfire events. This approach's goal is to strengthen long-term wildfire resilience by giving a scalable design for emergency response planning in Victoria.

Literature review

To begin searching for the best method to model the problem, we analyzed multiple articles answering similar problems. [21] analyzes drone communication using particle swarm optimization while [22] solves the same MCM problem using ant colony optimization. After analyzing our assumptions and approach to the problem, we decided to model over continuous time. Because ant colony optimization uses discrete time, we resorted to particle swarm optimization. [9], [23], and [15] all explain in depth what particle swarm optimization (PSO) is, how to implement PSO to a problem, and how PSO can be used to monitor forest fires. When analyzing fire area and fire spread rates, we used a dataset collected by Australia's government: [5]. This dataset was collected through a combination of different jurisdictions using a variety of methods such as aerial imaging, GPS-derived boundaries, and analyzing fire scars. Because this data is a combination of many subsets collected under different jurisdictions, there are possibilities of overlapping data due to the lack of regulating boundaries between each region. Because this data focused on the plains and mountainous regions of Victoria, we used [7] and [19] to estimate fire spread rates for urban areas. [19] used data collected from [10] to compare the sizes of different fires in urban areas, and their fire durations. They found many factors contributing to the differences in each fire including wind, infrastructure material and density. [7] also supported the same conclusions by collecting data using infrared scanning and automated fire clustering. Once enough data was collected to start implementing our PSO model, we used [18] to understand communication between different types of radios to conclude that only UHF range drones are necessary for our model and calculating the optimal distance between drones for sufficient communication.

3 Geographic Overview

3.1 Topography

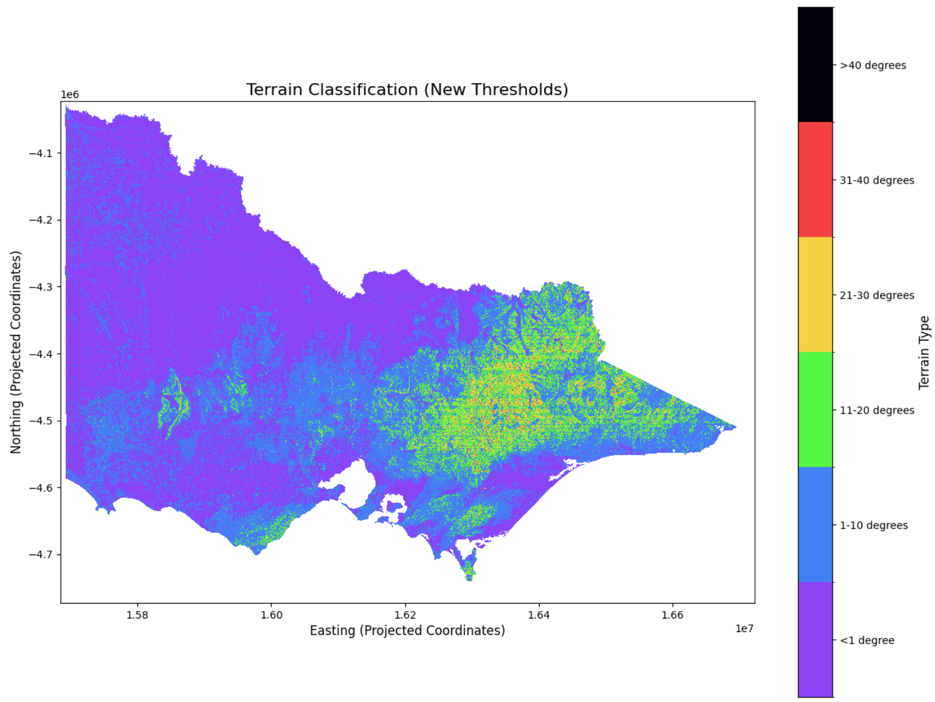

Figure 1: Terrain of Victoria

Cat 0: 51.71% **Cat 1:** 35.32% **Cat 2:** 9.60% **Cat 3:** 3.09% **Cat 4:** 0.27% **Cat 5:** 0%

Victoria's topography consists predominantly of flat and slightly sloped terrain with 87% of their land falling in Categories 1 (<1°) and 2 (1-10°) slope. The central and eastern regions contain the Great Dividing Range, the nation's largest mountain range, with inclines around 20°. Although these areas make up about 12% of the total land, areas with higher incline are critical for wildfire modeling because fires spread faster in these areas and are much harder to contain due to communication and movement limitations. Steep terrain clusters in the eastern region emphasize the necessity of having increased drone surveillance and repeater coverage to maintain communication with the EOC. We will discuss the source of the data and analysis later.

3.2 Fire Spread Model

The following model was used as an exploratory step in our wildfire analysis, but was not incorporated in the drone distribution model as we did not determine a good way to do this in the time span of this project. It was also an experiment in the use of Google's Antigravity AI manager tool to see how sophisticated of a model it could produce before we did our own work.

The model incorporates Victoria's topography and fuel types (water, urban, grassland, or forest). To determine the fuel types: urban regions are classified by proximity to the urban center (with slight, deliberate variation for populous cities and towns); water zones are those where the elevation is below 0 meters or one of four specific lakes and ports the agent identified; grassland regions are those with low elevation or small slope and moderate elevation; forest regions with high elevation or slope.

The different slopes and fuel types impact the rate at which the fire spreads according to rates determined by other research papers, including McArthur (1967)[16], Noble (1980)[17], and Cheney (1998)[2]. For instance, grassland fires can spread twice as fast as forest fires in extreme circumstances.

When the simulation begins, an initial wind direction is randomly selected at 20 m/s (72 km/h). Additionally, a random non-water location is selected as the ignition location. From there, the fire spreads according to the wind, topography, and fuel type. Additionally, the model represents ember spotting in forest bushfires, i.e. new fires can start downwind of the existing fire in forest regions. The simulation runs for a 14-day period and then terminates. As the wind and ignition location are randomly initialized, the simulation returns a different result every run.

The visualizer shows where the fire has spread to, how large it is, and the wind direction. Below are a couple of snapshots from one simulation:

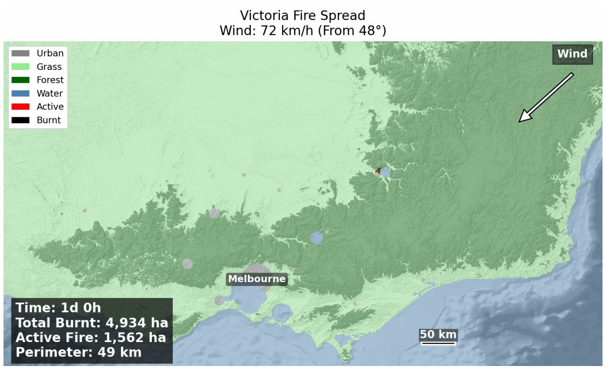

Figure 2: Simulation after 1 day

Figure 3: Simulation after 5 days

Figure 4: Simulation after 9 days

Figure 5: Simulation after 14 days

In this simulation, the fire starts in Wodonga, VIC, and spreads in the southwest direction. From the snapshots, you can see the fire spreads farther west, first, as the grassland burns far faster than the forest. After nine days, the fire has visibly spread around the forested area. Additionally, although the wind direction points southwest, the fire spreads northwest across the grassland because it is prone to burning. In the forest region, a keen eye can identify spot fires south of the front as firebrands fly through the forest.

While the simulation provides a visually appealing fire spread model, its critical flaw is the lack of firefighting activity or variable wind. A regular fire would not spread to nearly 1 million hectares (larger than Puerto Rico) in two weeks as firefighters would contain the flame to a much smaller area. So, this model demonstrates how a fire would spread throughout the state, but does not provide a working model to base drone placement off of.

3.3 Rate of Spread used in our Model

Our model, for simplicity, assumed a constant baseline rate of spread of fire in the plains and urban regions, which we assumed to be of constant elevation. Our baseline rate of spread is $v_{\text{ros}} = 1.47$ km hr^{-1}. This rate is was found using satellite detection in by a study called "Evaluating Australian forest fire rate of spread models using VIIRS satellite observations" by Matthew G. Gale and Geoffrey J. Cary (2025)[7]. Moreover, the same source also detailed different fire spread rates, such as in urban areas, where the average was closer to $v_{\text{ros}} = 2$ km hr^{-1}. Unlike flat areas however, mountain regions necessitated different spread rates based on the terrain differences. As the Department for Environment and Water states, every 10 degree increase in incline roughly doubles the spread rate [6]. All of these factors were considered while designing related models. Additionally, their research investigates the fire rate of spread in different types of vegetation coverage (Figure 6).

	N	Mean inferred ROS±SE (km hr^{-1})	Range (km hr^{-1})	Mean spread interval (min)
Dry Sclerophyll	48	1.48±0.17	0.20–4.49	56.8
Wet Sclerophyll	29	0.98±0.13	0.24–3.68	56.9
Eucalypt Woodlands	25	2.00±0.59	0.23–10.77	51.8
All observations	102	1.47±0.17	0.20–10.77	55.6

Figure 6: Summary statistics for VIIRS-derived inferred ROS observations in the major vegetation types investigated. SE indicates the standard error[7]

4 Assumptions and Limitations

4.1 Assumptions

- **Assumption:** No equipment loss for sending signal.
  - **Justification:** Priority is the configuration strategy regarding the drones and we consider that drones and other equipment are not damaged during use.
- **Assumption:** SSA drones and radio repeaters fly at the same height.
  - **Justification:** We consider both drones to fly at the same height to prevent the loss/weakening of signal between them.
- **Assumption:** The EOC is mobile.
  - **Justification:** Can move around the fire to ensure proper safety of the operators. This will also allow for a constant signal to be received from SSA and Radio-Repeater drones.
- **Assumption:** Fire expands in a circular shape.
  - **Justification:** Allows for strategy for drone deployment to stay consistent and creates an easier model to budget.
- **Assumption:** Constant rate of spread in plane (radius should not increase more than 3.5 km/hr).
  - **Justification:** Wind and other various fuel factors (infrastructure, humidity, etc) were not taken into consideration in our model due to model complexity.

- **Assumption:** Rate of spread doubles for every 10° increase in elevation for mountainous regions.
  - **Justification:** The increase in elevation causes an increase the rate of spread, so taking the average rate of change would allow consistency through mountainous regions.
- **Assumption:** Drones don't move when in air.
  - **Justification:** Drone movement creates a more complex drone strategy which would surpass our computational limits.
- **Assumption:** Only dealing with fires large enough to warrant drone usage.
  - **Justification:** There are constantly small fires happening throughout the Victoria that do not warrant the usage of drones and are beyond the scope of this project.
- **Assumption:** Only one bushfire is active at a time.
  - **Justification:** This simplifying assumption allows us to disregard cases where a drone's position could cover portions of 2+ fires' perimeters. We can also ignore seasonal risk in having several active fires around New Year's summer fire season.
- **Assumption:** Only using UHF (Ultra High Frequency) signals.
  - **Justification:** VHF (Very High Frequency) signals are too weak and everything including audio, video, etc can be transferred through UHF.
- **Assumption:** The plains and urban areas can be treated as 2D regions.
  - **Justification:** The change in elevation is negligible, and would not cause a significant rate of change in fire spread.

4.2 Limitations

4.2.1 Limitations of Historical Bushfire Boundaries dataset

1. Geoscience Australia is aware that duplicate data (features) may appear within this dataset. This duplicate data is commonly represented in the regions around state borders where it is operationally necessary for one jurisdiction to understand cross border situations. Care must be taken when summing the values to obtain a total area burnt.
2. The data within this aggregated national product is a spatial representation of the input data received from the custodian agencies. Therefore, data quality and data completion will vary.

4.2.2 Computational Limitations

The precision of our model was influenced by limitations on CPU usage and RAM. Google Colab, the platform used to code the Particle Swarm Optimization model had monthly limitations on monthly CPU usage, thus limiting the number of iterations the model can run and limiting the accuracy of our results. The particle swarm optimization simulation contains off-shore drones due to the computational limitations of our computer hardware. These offshore drones will be removed from our total budgeting plan manually. Moreover, limitations in RAM resulted in a low-resolution topographic map data, decreasing the precision of our solution. Topographic data does not take into consideration infrastructure (roads).

5 Methodology

5.1 Data Collection

5.1.1 Wildfire Data

Our model uses the data from the Historical Bushfire Boundaries dataset, published by the Digital Atlas of Australia [5]. The dataset includes the collection of data on burnt areas polygons supplied by different jurisdictional regions in Australia (Figure 7). The dataset contained two layers, one including data from Australia's Northern Territory Government for the first time, and one without. We used the layer that did not include Northern Territory information because our focus is on the region of Victoria, located in the Southeast of Australia.

Attribute name	Field Type	Description
fire_id	String	ID attached to fire (e.g. incident ID, Event ID, Burn ID).
fire_name	String	Incident name (if available).
ignition_date	Date	The date of the ignition of a fire event. Date and time are captured in jurisdiction local time and converted to UTC.
capt_date	Date	The date of the incident boundary was captured or updated. Date and time are captured in jurisdiction local time and converted to UTC.
extinguish_date	Date	The date a fire is declared safe (contained and under control). If available.
fire_type	String	Binary variable to describe whether a fire was a bushfire or prescribed burn.
ignition_cause	String	Cause of fire.
capt_method	String	Categorical variable to describe the source of data used for defining the spatial extent of the fire.
area_ha	Double	Burnt area in hectares. Calculated field so that all area calculations are done in the same map projection.
perim_km	Double	Burnt perimeter in kilometres. Calculated field so that all area calculations are done in the same map projection.
state	String	State custodian of the data. **NOTE**: Currently some states use and have in their feeds cross border data.
agency	String	Agency that is responsible for the incident.

Figure 7: Summary of variables provided by the Historical Bushfire Boundaries dataset

We used this dataset to calculate the statistics required for our model. This section includes a summary of the statistics calculated, the methods used, and where they are used in our model.

Data Preprocessing:

The first step in using any dataset is preprocessing the raw data. An important step in making the results derived from the Historical Bushfire Boundaries dataset applicable to our model, is to find a "modern cut-off" date. We seek to determine a year after which the data are representative of modern fire conditions. Wildfire regimes are non-stationary, meaning the factors that govern wildfire activity such as temperature, precipitation, vegetation growth, and firefighting responses change over time. Consequently, historical data that does not reflect current climatic and operational conditions is an unreliable guide for predicting wildfire behavior. To avoid this issue, we identify a cut-off year where conditions that contribute to wildfire behavior are consistent with present and near future conditions and restrict the analysis to data occurring after this threshold. This improves the reliability of future projections.

Finding a modern cut-off date:

The method we used to identify a modern cut-off date relied on finding a statistically significant shift in the average fire burn time data from 1899 to 2025. A shift in average fire burn time may be reflective of a shift in the climatic and operational conditions of wildfires. After filtering out the extreme outlier of the Black Saturday bushfire of 1939, a devastating fire which burned around 2 million hectares of land, we ran a change-point algorithm to detect potential cut-off dates.

```python
signal = filtered_burn_data['burn_time'].values
model = "l2"
algor = rpt.Pelt(model=model).fit(signal)
#indices in the signal array
change_points = algor.predict(pen = 900000)
#The years corresponsing to the change points, excluding last in list because that is not
#a data point
potential_cutoffs = yearly_mean_burn['year'].iloc[change_points[:-1]].values
print("Potential cut-off years: ", potential_cutoffs)
```

Listing 1: Algorithm for identifying change points in burn time data

Listing 1 shows the python code snippet from analysis.py that was used to identify potential cut-off dates. The algorithm uses the rupture library in Python and a least-squares (l2) loss model to detect regime shifts in average fire duration. The output of the code snippet is as follows:

```
Potential cut-off years:  [1938 1944 1949 1954 1969 1974 1989 2004]
```

The next step is to determine if any of these potential cut-off points are statistically significant using a z-test. Since 2004 is the most recent potential cut-off point, it has a higher change of being indicative of a shift to modern data. Therefore, we used a two-sample z-test to determine whether the mean burn duration of fires differed significantly before and after 2004. The null hypothesis is $H_0 : \mu_b = \mu_a$ where μ_b is the population mean of the burn durations before 2004 and μ_a is the population mean of the burn durations after 2004. The z-test program, located in modern_analysis.py, produced a z-statistic of z = 2.33 and a p-value of p = 0.020. Since the $p \leq .05$, we reject the null hypothesis. Therefore, the mean burn-durations are significantly different after 2004, and we can use this year as our modern cut-off date.

Calculations:

The average burn time of small fires (2,000-10,000 ha) and large fires (10,000 ha or greater) is necessary to calculate the total 10 year cost of maintaining the CFA drone force. The average burn times were calculated in burn_analysis.py. The method is straight-forward. First, split the data into small fires and large fires based on their areas. Then, create a new column containing the burn time of each fire by finding the difference between the the extinguish and ignition date. Finally, use the newest burn-time column to calculate the respective averages of burn times of small and large fires. However, complication arises because although both timestamps are documented as Coordinated Universal Time (UTC) in the Historical Bushfire Boundaries dataset, the raw data encodes them inconsistently (timezone-aware versus timezone-naive), requiring normalization before analysis. Listing 2 shows the necessary lines of code to resolve the time-zone conflict, by forcing ignition_date and extinguish_date to be time-zone naive.

```python
fire_data = gpd.read_file(gdb_path, layer = layer_name)

fire_data['ignition_date'] = pd.to_datetime(fire_data['ignition_date'], errors='coerce', utc=True)
fire_data['capture_date'] = pd.to_datetime(fire_data['capture_date'], errors='coerce', utc=True)
fire_data['extinguish_date'] = pd.to_datetime(fire_data['extinguish_date'], errors='coerce', utc=True)

fire_data['ignition_date'] = fire_data['ignition_date'].dt.tz_localize(None)
fire_data['extinguish_date'] = fire_data['extinguish_date'].dt.tz_localize(None)
```

Listing 2: Code to fix time zone conflict

The average burn time of small fires was calculated to be approximately 684 hours, and the average burn time of large fires was calculated to be approximately 851 hours.

The program named analysis.py provides an overview of fire behavior statistics in Australia and in Victoria. Tables 1 and 2 provide a summary of the statistics calculated in analysis.py. Figures 8-10 are scatter plots generated by analysis.py. The program named analysis2.py provides an overview of fire behavior statistics in Australia and in Victoria, but limited to the modern dataset 2005-2025. Tables 3 and 4 provide a summary of the statistics calculated in analysis2.py. The program also provides a scatter plot of yearly fire frequency in Australia and the frequency of extreme fire events, which are not shown. Not all the statistics calculated were incorporated in our model, but the statistics provided give a general overview of fire behavior in Australia and Victoria, and are a useful resource for others who are interested in researching fires in Australia. All code and datasets can be found in the GitHub repositories and Google Drive, and all statistics and plots can be replicated.

Statistic	**Result**
`Number of fire polygons`	345,345
`Total area burned`	346,461,262 ha
`Mean fire area`	1,003.2 ha
`Max fire area`	5,763,897 ha
`Min fire area`	0 ha
`Fire Frequency by Year`	Run analysis.py to view output
`Fire Frequency by State and Year`	Run analysis.py to view output

Table 1: Fire behavior statistics, entire Australia, 1899-2025

Statistic	**Result**
`Mean burn time`	231.0 hr
`Max fire area`	87,744 hr
`Min fire area`	0 hr

Table 2: Fire burn statistics, entire Australia, 2005-2025

Statistic	**Result**
`Total area burned`	204,882,570 ha
`Mean fire area`	1,155.7 ha
`Max fire area`	2,769,613 ha
`Min fire area`	0 ha
`Fire Frequency by Year`	Run analysis2.py to view output
`Fire Frequency by State and Year`	Run analysis2.py to view output

Table 3: Fire behavior statistics, entire Australia, 2005-2025

Statistic	Result
`Number of Fires`	72,618
`Total area burned`	7,114,275 ha
`Mean fire area`	98.0 ha
`Max fire area`	892,046 ha
`Min fire area`	0 ha
`Fire Frequency by Year`	Run analysis2.py to view output

Table 4: Fire behavior statistics, Victoria region, 2005-2025

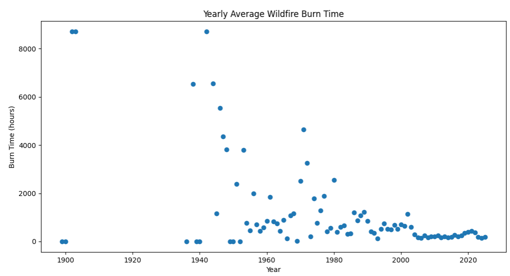

Figure 8: Scatter plot of yearly average wildfire burn times, Australia, 1899-2025, excluding Black Saturday outlier year

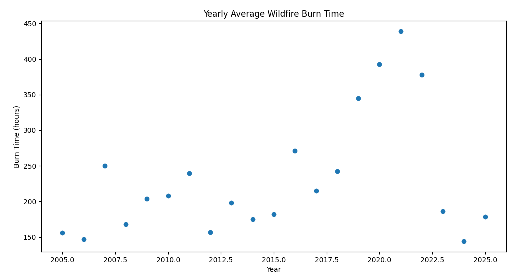

Figure 9: Scatter plot of yearly average wildfire burn time, Australia, 2005-2025

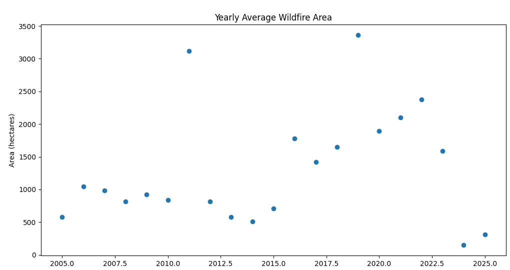

Figure 10: Scatter plot of early average wildfire area, Australia, 2005-2025

5.1.2 Topographic Data

We gathered the topographic data of Victoria, Australia, from CeRDI, which has extensive data on the topography of Australia and other land related data. The downloaded file was a 2.86 GB .tif file with 30 meter resolution, which was deemed sufficient for our purposes, balancing compute requirements and resolution.

Initially, we formalize the input of the topographic data by extracting the elevation data from the file to calculate the slope, $\tan^{-1}(\sqrt{x_r^2 + y_r^2})/2$, where r denotes resolution. To ensure the integrity of the data we worked with, we also eliminated any NaN and out of bounds data.

All terrain-related grids have shape $(\text{rows}, \text{cols})$ and are used to compute fire-weighted, slope-adjusted coverage. Below outlines some other variables we used to process the data and to feed into the drone formation models.

Variable	Description
`elevation_data_processed`	Terrain grid of size (rows × cols)
`slope_degrees`	Derived slope at each pixel
`pixel_width_meters`	Horizontal pixel resolution (m/pixel)
`fire_risk_weight`	Fire spread risk per pixel
`valid_terrain_mask`	Mask of finite, valid terrain pixels

Table 5: Terrain-related variables that we calculated to generate the map.

5.1.3 SSA & Radio Repeater Range

Terrain Type	Repeater Range (km)	Ground Personell Radio Range (km)
Plains	12	5
Urban	6	2
Mountain	3	1

Table 6: Radio Repeater and Ground Communication Range by Terrain Type

SSA and Radio Repeater ranges were calculated by using experimental data from the United States National Telecommunications and Information Administration and combination of line-of-sight geometry and the radio horizon formula. In the experiment, systems operating in the UHF band (1 GHz) showed losses of approximately 10.6 dB at 30 m, 16.4 dB between 30-90 m, and 22.3 dB beyond 90 m. These height thresholds are used to categorize our terrain types: plains, urban, and mountainous terrains. When there's perfect line-of-sight and flat terrain, the maximum communication distance is approximated using the radio horizon formula:

$$d_{ideal} \approx 3.57(\sqrt{h_1} + \sqrt{h_2})$$

where $h_1 = 2m$ is the ground radio height and $h_2 = 100m$ is the drone altitude. This allows for an ideal repeater range of 40 km. To account for terrain-induced range loss, we applied a range reduction factor:

$$\text{Range Reduction Factor} = 10^{L_{extra}/20}$$

where L_{extra} is the additional path loss in decibels. The communication range is shown as $d_{actual} = d_{ideal}/\text{Range Reduction Factor}$. Applying these formulas results in the corresponding repeater ranges: 12 km for plains, 6 km for urban terrain, and 3 km for mountainous.

5.2 Variables

5.2.1 Inputs

Category	Variable/Functions	Description
Fire		
	$A(t)$	Fire area (km^2)
	$R(t)$	Fire radius (km)
	v_{ros}	Rate of spread (km/hr)
	θ	Terrain slope angle (degrees)
Drone	r_s	Surveillance coverage radius per SSA (10 W, km)
	r_r	Repeater coverage radius per Repeater (10 W, km)
	$C_s = \pi r_s^2$	Coverage area per SSA (km^2)
	$C_r = \pi r_r^2$	Coverage area per Repeater (km^2)
	T_{end}	Drone endurance (2.5 hrs)
	p	Fraction of time a drone is airborne
Batteries	$D_{c,l}, D_{c,s}$	Battery charging hours (large/small)
	$S_{c,l}, S_{c,s}$	Drone charges (large/small)
Topography	$E(i,j)$	Elevation at pixel (i,j)
	r	Pixel spatial resolution (m/pixel)
Particle Swarm Optimization	N_s	Number of SSA drones
	$x_i(t), v_i(t)$	Position/velocity of SSA drone i at iteration t
	p_{best_i}, g_{best_i}	Personal/global best position of drone i
	w	Inertia weight
	c_1, c_2	Cognitive and social coefficient
	r_1, r_2	Uniform random variables in $(0,1)$
	J	PSO objective (cost) function
	$\mathbf{x} = (x_i, y_i) \in \mathbb{R}^{200}$	Decision vector
Minimal Spanning Tree	S	Set of SSA drone locations
	r_r	Communication radius constraint
	N_r	Maximum repeater drone budget
	$c(p,q)$	Repeater distance function between points p, q

5.2.2 Outputs

Category	Variable/Function	Description
Topography		
	$S(i,j)$	Slope at pixel (i,j)
Drone	N_s	Number of SSA drones
	N_r	Number of Radio Repeater drones
	N_t	Total number of drones
	$\{x_i^*, y_i^*\}$	Optimal SSA drone positions
	J^*	Minimum PSO objective value
	N_{conn}	Number of connected SSA drones
	$F_{h,l}$	Large fire hours
	$F_{h,s}$	Small fire hours
Cost	$E = 2.4(S_{c,l})(8) + 2.4(S_{c,s})(4)$	Equipment charging cost
	$P = \frac{10{,}000(N_s+N_r)}{p} + 10E$	Total price

5.3 Drone Optimization Algorithm

Part 1: Particle Swarm Optimization

5.3.1 Particle Swarm Optimization Strategy

Particle Swarm Optimization (PSO) is an optimization algorithm that iterates through candidate solutions, often to minimize or maximize some function. Such functions of interest could be the formation of humans to find maximum amounts of treasure or flocking of birds to ensure equal resource splitting.

A similar algorithm to PSO is the Ant Colony Algorithm. Although the variables within Ant Colony Algorithm are often discrete, PSO uses continuous variables. Our problem involves finding the optimal location of drones over different areas, different terrain, and different fire spread rates. Moreover, our goal is to get the best coverage of the fire area without using redundant drones, which would have the greatest flexibility if the drones could move freely in space. With the references of [9], [13], [15], [20], and [23], we have formulated the PSO algorithm stated below.

5.3.2 Parameters and Functions

The PSO algorithm uses 3 main functions: the velocity update function, position update function, and the cost function.

Let $x_i(t) \in \mathbb{R}^2$ denote the position of drone i at iteration t, and let $v_i(t)$ denote its velocity. Then, the position update rule

$$x_i(t+1) = x_i(t) + v_i(t+1). \tag{1}$$

The velocity update rule is

$$v_i(t+1) = w\, v_i(t) + c_1 r_1 \big(p_{\text{best},i} - x_i(t)\big) + c_2 r_2 \big(g_{\text{best}} - x_i(t)\big), \tag{2}$$

where $r_1, r_2 \in (0,1)$ are independent random variables. The quantities $p_{\text{best},i}$ and g_{best} represent the personal best position found by drone i and the global best position found by the swarm, respectively.
The hyperparameters used in the velocity update equation are defined as follows:

- w (inertia weight): controls momentum and exploration of the search space;
- c_1 (cognitive coefficient): attracts particles toward their personal best locations;
- c_2 (social coefficient): attracts particles toward the global best solution.

To prevent particles from making unrealistically large movements across the terrain, we impose a velocity clamp that limits the magnitude of $v_i(t)$ at each iteration.

The PSO algorithm minimizes a scalar objective function J, which encodes surveillance quality, redundancy, and terrain-dependent fire risk:

$$J = -R_{\text{cov}} + P_{\text{overlap}} + P_{\text{uncovered}} \tag{3}$$

Where

- R_{cov} denotes the fire-risk-weighted effective coverage achieved by the drones by incorporating both terrain slope and fire spread dynamics, weighting each covered pixel according to its estimated fire spread rate and an effective coverage factor proportional to cos(slope). ;
- P_{overlap} penalizes redundant coverage where multiple drones observe the same terrain pixel;
- $P_{\text{uncovered}}$ penalizes high-risk terrain pixels that are not covered by any drone.

5.3.3 Applying the Particle Swarm Optimization

We optimize the planar coordinates (x, y) of N_s drones.
The total dimensionality of each particle is

$$\dim = 2 \cdot N_s.$$

Each particle position vector is given by

$$\mathbf{x} = (x_1, y_1, x_2, y_2, \ldots, x_{100}, y_{100}) \in \mathbb{R}^{200}.$$

The PSO hyperparameters are:

$$\begin{aligned} w &= 0.9 \quad \text{(inertia weight)}, \\ c_1 &= 1.5 \quad \text{(cognitive coefficient)}, \\ c_2 &= 1.3 \quad \text{(social coefficient)}. \end{aligned}$$

Those parameters were found to yield the least number of drones on the ocean, which we will discuss later. On the other hand, particle velocities are clamped as

$$v_{\text{clamp}} = \left[-0.05(x_{\max} - x_{\min}),\ \ 0.05(y_{\max} - y_{\min})\right],$$

preventing excessively large jumps across the terrain (capped at 5 percent of terrain width/height). This helped the particles iterate at a faster speed, which is necessary at low number of iterations (20).

5.3.4 Drone Strategies

To account for geographic heterogeneity of Victoria, we considered 3 major terrain categories: urban areas, plains, and mountainous regions. Urban areas and plains exhibit negligible elevation variation and are therefore treated as flat terrain, while mountainous regions exhibit significant elevation gradients that substantially affect fire spread rate. Our research suggests that fire spread rates approximately double for every 10° increase in slope angle. Consequently, mountainous regions require denser drone coverage to achieve comparable surveillance effectiveness (as previously shown with the radio ranges). These terrain-dependent effects are directly incorporated into the objective function through the fire risk weighting and effective coverage terms. To evaluate the robustness and edge cases of the optimization framework, plains are treated as the best-case scenario, urban areas as a moderate case, and mountainous terrain as the worst-case scenario.

1. Urban: 1.47 km/hr spread rate.
2. Plains: 2 km/hr spread rate.
3. Mountains: 1.47 km/hr spread rate with slope-amplified spread effects (using cosine of slope, appropriately, to model the objective function).

Part 2: Minimal Spanning Tree Algorithm

5.3.5 Connecting SSA Drones Using MST

Since the optimal SSA drone formations have been calculated from the PSO, we follow up by filling as many signal gaps between each SSA drone as possible. We employ a Minimal Spanning Tree (MST) algorithm because, analogous to our problem, MSTs uses the least number of edges to connect the greatest amount of nodes. We use an algorithm that is based on the same principles as Prim's Algorithm, as detailed in [8], however we have made significant modifications to adapt differences in edge length.

Let $S = \{s_1, \ldots, s_N\} \subset \mathbb{R}^2$ denote the set of SSA drone locations. Each drone has a fixed communication radius r_r that is previously defined. Two nodes can directly communicate if their Euclidean distance does not exceed r_r. If $d(s_i, s_j) > r_r$, communication may be achieved by inserting intermediate repeater drones along the straight-line path between the two nodes. A global budget N_r limits the total number of repeater drones that may be deployed.

Distance function/pseudometric. We define the distance function between any two points $p, q \in \mathbb{R}^2$ as

$$c(p,q) = \begin{cases} 0, & \|p-q\| \leq r_r, \\ \lceil \|p-q\|/r_r \rceil - 1, & \text{otherwise.} \end{cases}$$

which corresponds to the minimum number of intermediate nodes required to ensure communication between SSA drones. The network is then constructed using a greedy expansion strategy similar to Prim's algorithm, with edge weights given by the repeater cost $c(\cdot,\cdot)$.

Initialization. The geometric center of the spatial domain is computed, and SSA drones are sorted by increasing distance to this center. The most central SSA drone initializes the network:

$$\mathcal{N}_\prime = \{s_{i^\star}\}.$$

Iteration. At iteration t, let $\mathcal{N}_\sqcup$ denote the set of nodes currently in the network (both SSA drones and repeaters), and let $U_t = S \setminus \mathcal{N}_\sqcup$ be the set of unconnected SSA drones. The algorithm selects

$$s^\star = \arg\min_{s \in U_t} \min_{n \in \mathcal{N}_\sqcup} c(s,n),$$

and connects $s^\star$ to the network provided that the cumulative repeater count does not exceed N_r. If $c(s^\star, n^\star) = k > 0$ repeaters are required to connect $s^\star$ to its closest network node $n^\star$, repeater positions are deterministically placed as

$$r_i = s^\star + i r_r \cdot \frac{(n^\star - s^\star)}{\|n^\star - s^\star\|}, \quad i = 1, \ldots, k.$$

Each repeater is added to $\mathcal{N}_t$, allowing subsequent SSA drones to connect through previously placed repeaters. The algorithm then terminates when either all SSA drones are connected or no remaining SSA drone can be connected without exceeding the repeater budget N_r.

To implement the algorithm efficiently, we utilized NumPy for its quick array operations.

5.4 Changing Likelihood of Extreme Fire Events

5.4.1 Extreme Fire Frequency

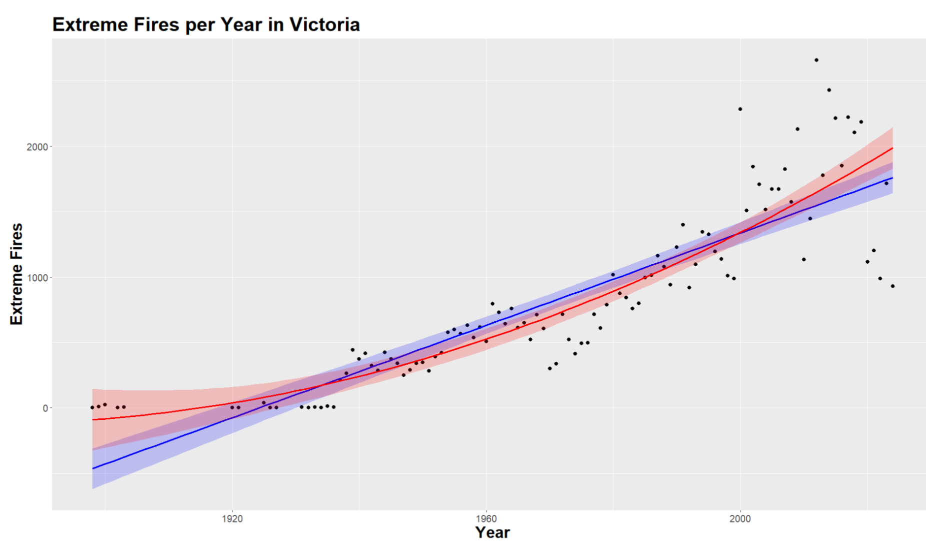

Figure 11: Scatterplot of yearly extreme fire frequency, with a second degree polynomial regression curve (red) and linear regression line (blue) with their 95% confidence intervals of coefficient *Year*.

In the 21st century the effects of climate change on extreme weather events has been a pressing concern by scientists. As carbon dioxide into the atmosphere increases, global temperatures rise, leading to higher temperature and greater risk for fire. According to Australia's Climate Council, "Since the mid-1990s, southeast Australia has experienced a 15% decline in late autumn and early winter rainfall and a 25% decline in average rainfall in April and May" [4]. As a result, Australian conditions are drier and hotter, increasing the risk of extreme fire events. In Australia, the Forest Fire Danger Index (FFDI) is used to measure the degree of risk of fire in forests [14]. The index has a scale from 0 to 100, with fires between 75 and 100 defined as 'extreme.' Following the same convention of splitting at the 75th percentile, we defined "extreme fire events" as all fires in which the area is in the top 75th percentile. Using the Bushfire Historical Extents dataset, we filtered out all of the fires with areas that were not in the 75th percentile, and then plotted the frequency of extreme fire events in Australia over time (Figure 11). The regression curves show that the frequency of extreme fire events has increased since the 20th century. The positive trends between extreme fire event frequency and time shows that the extreme fire event frequency is likely to continue increasing in the long-term future. Our objective is to determine how many additional drones Victoria's Country Fire Authority (CFA) needs to purchase, if any, to adapt to the changing likelihood of extreme fire events over the next decade. It is important to note that not all extreme fire events are large enough to warrant the use of drone and can be handled by firefighter personnel. Only the largest of fires (critical fires) necessitate the deployment of the CFA drone fleet. Our team determined critical fires to be those with areas 2,000 hectares or greater. We will attempt to model changes in the frequency of critical fires using regression analysis and use this to inform our decision of additional drones needed. Figures 12 & 13 shows the frequency of critical fires over the past 20 years, the modern era of firefighting. Because wildfire regimes are non-stationary, it is necessary to restrict the analysis to data that is representative of modern fire conditions. Inclusion of earlier data may bias projections if historical fire regimes differ significantly from those of the present and near future (see section 5.1.1 Wildfire Data for determining a modern cut-off date).

5.4.2 Interpretation of the Model

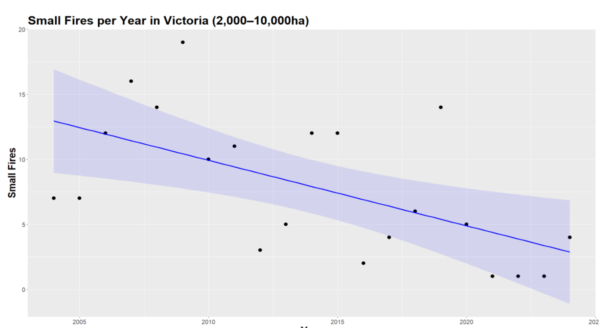

Figure 12: Small fires per year with linear regression line and 95% confidence interval.

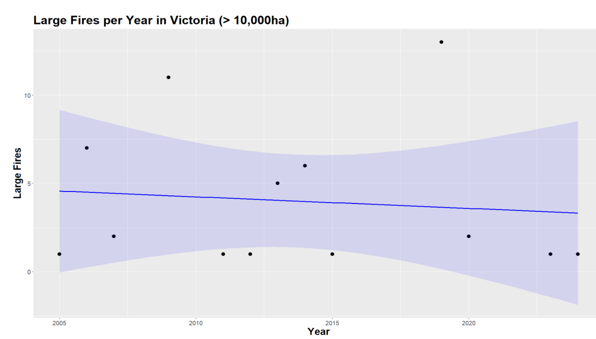

Figure 13: Large fires per year with linear regression line and 95% confidence interval.

Coefficients	**Estimate**	**Std. Error**	**t value**	**Pr**$(>\|t\|)$
(Intercept)	1022.7515	327.2656	3.125	0.00557 **
Year	-0.5039	0.1625	-3.101	0.00588 **

Signif. codes: 0 '***' 0.001 '**' 0.01 '*' 0.05 '.' 0.1 ' ' 1

Residual standard error: 4.509 on 19 degrees of freedom
Multiple R-squared: 0.336, Adjusted R-squared: 0.3011

Table 7: Linear regression output, small fires

Coefficients	Estimate	Std. Error	t value	Pr(> $\|t\|$)
(Intercept)	135.48380	397.96679	0.34	0.740
Year	-0.06529	0.19763	-0.33	0.747

Residual standard error: 4.306 on 11 degrees of freedom
Multiple R-squared: 0.009826
Adjusted R-squared: -0.08019

Table 8: Linear regression output, large fires

The linear regression line shown in Figure 12 has a slight negative trend while the regression line shown in 13 has a flat trend. With a coefficient of -0.5039 and a p-value of approximately 0.059 for the *Year* parameter in the small fires and a coefficient of -0.063 and p-value of .747 for large fires, there is statistically significant evidence that there is a decrease in small fires (2000-10,000ha) and no statistically significant evidence for a decrease or increase in large fires throughout the last 20 years. The R^2 value of .336 indicates a weak fit for the negative trend line and explains that the model captures some of the variance in the data. The high variance, weak predictive ability of regression lines outside their bounds, and conflicting evidence in our year-over-year data suggests that we cannot conclude an increase or decrease in small and large fire events. Therefore, the purchase of additional drones to respond to changing likelihood of extreme fires in the next 10 years due to climate change is not warranted.

6 Solution

We evaluated the particle swarm optimization algorithm using the existing PySwarms library in Python. We ran 20 iterations using the aforementioned parameters, which yield a minimum cost of $2.59 * 10^{11}$. The positions of the SSA's are then displayed in white, with its range displayed in a circle around it. After the ideal drone formations were calculated, the coordinated were saved in a NumPy array, where we calculated the minimal spanning tree connecting as many SSA Drones as possible. We chose the center of each map due to the difficult nature of EOC's reaching there, and we iterated through the SSA drones as described in the MST algorithm. Plotting the results using Matplotlib yields the following results:

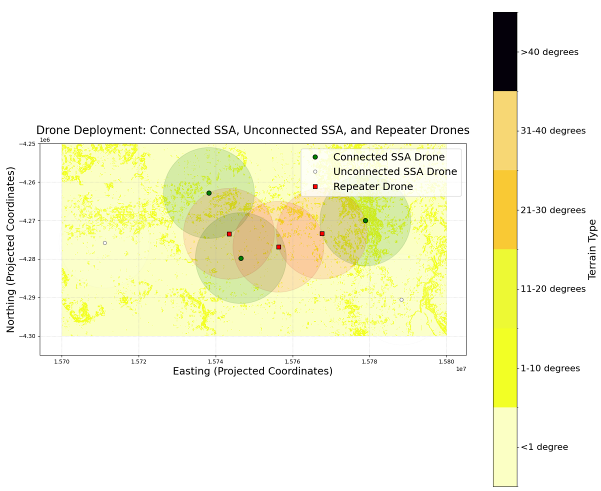

Figure 14: Total connected SSA drones: 5. Total repeater drones used: 3. Remaining SSA drones (unconnected): 2. Drone Network (SSA + Repeater): 6. Total drones (SSA + repeaters) : 8.

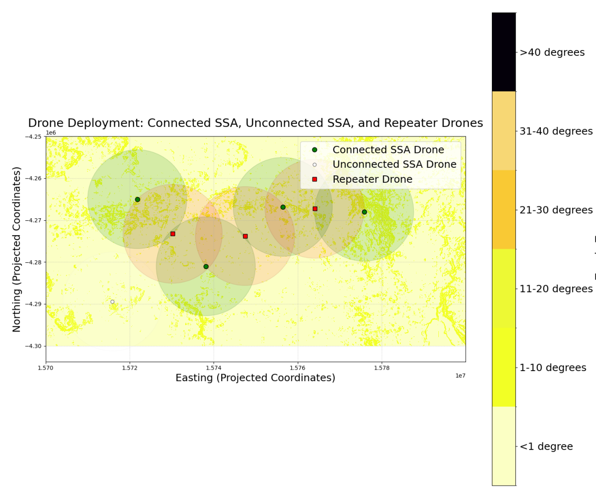

Figure 15: Total connected SSA drones: 4. Total repeater drones used: 3. Remaining SSA drones (unconnected): 1. Drone Network (SSA + Repeater): 7. Total drones (SSA + repeaters) : 8.

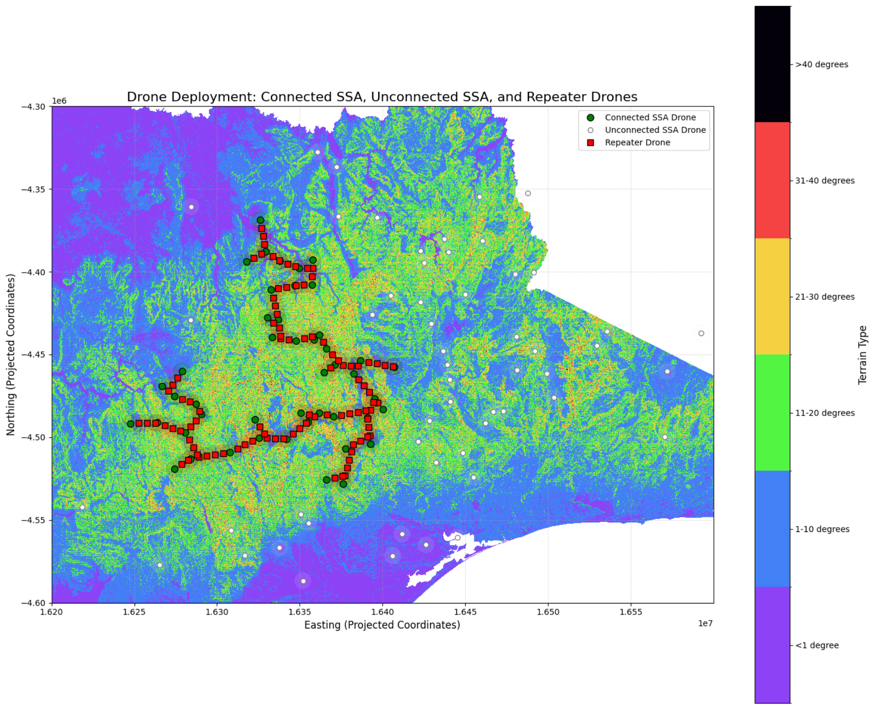

Figure 16: Total connected SSA drones: 46. Total repeater drones used: 96. Remaining SSA drones (unconnected): 54. Connected drone fleets: (SSA + Repeaters): 142. Total: 194 in the air (+2 on ocean, which are ignored)

7 Budget

7.1 Drone Amount Calculations

A single drone alternates between flight and recharge. The total cycle time is

$$T_{\text{cycle}} = 2.5 \text{ hr} + 1.75 \text{ hr} = 4.25 \text{ hr}.$$

The fraction of a cycle during which a drone is airborne is

$$p = \frac{2.5}{4.25} = \frac{250}{425} = \frac{10}{17}.$$

To maintain 194 drones airborne at all times, the total number of drones N must satisfy

$$N \cdot p = 194.$$

Solving for N, we obtain

$$N = \frac{194}{p} = 194 \cdot \frac{17}{10} = \frac{3298}{10} = 329.8.$$

Since the number of drones must be an integer, we round up:

$$N = 330.$$

7.2 Total 10 Year Cost Calculation

The amount of upfront costs is strictly the drones.

$$N_t \cdot 10{,}000 = 330 \cdot \$10{,}000 = \$3{,}300{,}000$$

The equipment charging cost is calculated as follows.

$$\begin{aligned}
&F_{h,l} = 851 \\
&F_{h,s} = 684 \\
&D_{c,l} = 51 \cdot 194 = 165{,}094 \\
&D_{c,s} = 684 \cdot 8 = 5{,}472 \\
&S_{c,l} = 165{,}288/2.5 = 66{,}037 \\
&S_{c,s} = 5{,}472/2.5 = 2{,}188 \\
&E = 2.4(66{,}037)(4) + 2.4(2{,}188)(8) = \$306{,}176
\end{aligned}$$

Total budget needed over 10 years.

$$P = 10{,}000(330) + 10(306{,}176) = \$6{,}361{,}760$$

7.3 Annotated Budget Request

Drones	**$3,300,000**
330 drones; the maximum number of drones required for Victoria according to our model.	
Electricity allowance	**$3,061,760**
The expected electricity cost to charge the drones for use over 10 years, without adjusting for inflation.	
Total:	**$6,361,760**

Under our assumptions (Section 4), the model predicts we would need 330 drones for continual coverage of Victoria's worst fires.

8 Model Evaluation and Conclusion

Our model, using the Particle Swarm Optimization, provides a method to minimize the number of drones and maximize the coverage, making it a cost-efficient solution for responding to critical fires with drones. Our model also effectively distinguishes fires into small, nearly flat fires, and large, sweeping fires. One of our models strengths lies in how it considers the influence of topography on the rate of spread and radio range. Our model provides insight on how to efficiently respond to wildfires fires using drones, providing a working model of Particle Swarm Optimization that can be replicated with different parameters for different regions.

However, the model output of our Particle Swarm Optimization places two drones in the ocean due to limitations in the amount of iterations we could run. This is a weakness in our proposed drone distribution. Additionally, the accuracy of our cost estimations may have been negatively impacted by skewed statistical calculations on average burn times. The Historical Bushfire Boundaries dataset included prescribed (planned) burns, which were not filtered out prior to statistical calculations.

Future iterations of this model may improve by factoring in the influence of wind and weather patterns on drone flight and fire spread, such as using the model presented in section 3.2. The baseline average rate of spread $v_{\text{ros}} = 1.47$ km hr^{-1} calculated by Gale and Cary incorporates the influence of wind speeds, but our model does not allow for the simulation of drone placement under different weather conditions. Adding this function to our model would make this model more useful for Fire Departments who require real-time information on optimal drone placements to respond to fires. Another way to improve our model would be to take into consideration the mobility of drones. Our model, for simplicity, assumes drones to be stationary, likely leading to an overestimation of the drones needed to cover a fire area. If drones can move fast enough to cover multiple areas without leading to major gaps in surveillance or communication, incorporating drone mobility into our model could reduce the amount of drones needed in our solution, and lower the cost of operations.

Overall, the model incorporates historical bushfire data, Victoria's topography, communication constraints, and optimization techniques to find answers to all four aspects of Victoria's Country Fire Authority's problem. The two-method model distributes drones according to their respective objective. The data showed that the wildfire events under our consideration are not becoming more frequent and that the initial number of drones would be sufficient to monitor fires over the next ten years. Our budget analysis showed that the drone program would cost a modest $6 million for equipment. We believe the drone program is a cost-efficient way to provide better surveillance of the bushfire and allow for a more coordinated response, and are in favor of the program.

9 Acknowledgments

We would like to acknowledge Professor Mason Porter for his assistance working through the PSO model design.

10 AI Use Report

We used AI as a coding tool to supplement the facts and figures research we had conducted. The fire spread model in Section 3.2 was constructed entirely through AI scripting in Python. The rest of the code was mostly hand-written with AI used for debugging purposes (including efficiency enhancements of the code in the PSO section via vectorized objective function, out of bounds check, and deleting unnecessary parts of the code). We additionally used AI to help format this document appropriately. Besides 3.2, all of the model selections and implementations were hand-picked, not AI suggestions. AI spellcheck was used, but not to rewrite any sections of this document. Models/interfaces used: ChatGPT 5.1, Gemini 3, Antigravity-1.11.14, Writefull.

11 Contributions

Lily C: Worked on statistical analysis, processing, and interpretation of raw data from Historical Bushfire Extents dataset by writing several programs: analysis.py, analysis2.py, frequency_predictions.py, modern_analysis.py, burn_analysis.py. Wrote parts of the Data Collection section. Researched a baseline fire spread rate to use for our model. Analyzed the the changing liklihood of extreme fires due to climate change. Wrote parts of the the limitations section and the evaluation of the model section.

AJ F: Worked on the budget analysis, processing of statistical models, topographic data explanation, bibliography, and formatting/outline of the report. Helped in creation of the budget equation and writing of statistical model interpretation.

Frank H: I worked on parts of the introduction, fire spread model, parts of the assumptions list, parts of the model evaluation, parts of the budget analysis, parts of the conclusion, Acknowledgments, and AI Use Report. I brought ground knowledge about bushfire season in Australia and some intuition for the Dividing Range being the nexus of Victoria's fires.

Reina S: I researched the typ of model we wanted to use and came to the conclusion that particle swarm optimization would be best for this problem. I also helped alter Da-Yi's model for optimizing the number and locations of ssa and repeater drones from the 3D model to the 2D model, and created the respective visualizations. Then I added to our list of assumptions, and described our inspiration and how we used our data in the literature review.

Da-Yi W: Finding and analyzing topographic data (terrain/elevation), 3D model of the particle swarm optimization, greedy algorithm for the repeater formation. For the overlead, I also worked on finding the total number of drones needed to keep all 194 drones running continuously, and parts of the topographic overview, assumptions list, variables, PSO, MST, solution, and all code/math for the topography processing, 3D PSO, and MST.

12 Code Repository

Our code has all been uploaded to GitHub here: `https://github.com/20wudy/Math_142_Wildfire_code`.

References

[1] Brunson, L. (n.d.). *Assessment of compatibility between ultrawideband devices and selected federal systems*. National Telecommunications and Information Administration. https://www.ntia.gov/files/ntia/publications/uwb.pdf

[2] Cheney, N. P., Gould, J. S., & Anderson, W. (1998). Prediction of fire spread in grasslands. *International Journal of Wildland Fire*. https://doi.org/10.1071/WF9980001

[3] Climate Change in Australia. (n.d.). *Download datasets*. https://www.climatechangeinaustralia.gov.au/en/obtain-data/download-datasets/

[4] Climate Council. (2019). *This is not normal: Climate change and escalating bushfire risk*. Climate Council. https://www.climatecouncil.org.au/wp-content/uploads/2019/11/CC-nov-Bushfire-briefing-paper.pdf

[5] Commonwealth of Australia. (n.d.). *Bushfire historical extents* [Dataset]. Digital Atlas of Australia. https://digital.atlas.gov.au/datasets/524e2962bd8b4968b8df9f9774345926/about

[6] Department for Environment and Water. (n.d.). *The science behind fire behavior*. Government of South Australia. https://www.environment.sa.gov.au/topics/fire-management/fire-science-and-planning/fire-behaviour

[7] Gale, M. G., & Cary, G. J. (2025). Environmental modelling and software. *Environmental Modelling & Software*. https://doi.org/10.1016/j.envsoft.2025.106436

[8] GeeksforGeeks. (2025). *Prim's algorithm for minimum spanning tree (MST)*. https://www.geeksforgeeks.org/dsa/prims-minimum-spanning-tree-mst-greedy-algo-5/

[9] GeeksforGeeks. (2025). *Particle swarm optimization (PSO): An overview*. https://www.geeksforgeeks.org/machine-learning/particle-swarm-optimization-pso-an-overview/

[10] Hamada, M. (1977). *Architectural fire resistant themes* [In Japanese]. Kenchikugaku Taikei. https://nrifd.fdma.go.jp/publication/gijutsushiryo/gijutsushiryo_01_40/index.html

[11] Himoto, K., & Tanaka, T. (2008). Development and validation of a physics-based urban fire spread model. *Fire Safety Journal*. https://www.sciencedirect.com/science/article/pii/S0379711207001257

[12] Kazhykarim, Y. (n.d.). *ScholarWorks @ UTRGV*. https://scholarworks.utrgv.edu/

[13] Kazhykarim, Y. (2020). *Topography estimation using particle swarm optimization* (Master's thesis, University of Texas Rio Grande Valley). ScholarWorks @ UTRGV. https://scholarworks.utrgv.edu/cgi/viewcontent.cgi?article=1488&context=etd

[14] Luke, R. H., & McArthur, A. G. (1978). *Bushfires in Australia*. Department of Primary Industry, Forestry and Timber Bureau, Commonwealth of Australia.

[15] Luo, Z., et al. (2025). Forest fire monitoring UAV system using forest PSO-GA algorithm. *Preprints*. https://www.preprints.org/manuscript/202502.0436/v1

[16] McArthur, A. G. (1967). *Fire behaviour in eucalypt forests*. Victorian Government Library Service. https://www.vgls.vic.gov.au/client/en_AU/vgls/search/detailnonmodal/ent:$002f$002fSD_ILS$002f0$002fSD_ILS:643141/one

[17] Noble, I. R., Gill, A. M., & Bary, G. A. V. (1980). McArthur's fire-danger meters expressed as equations. *Australian Journal of Ecology*. https://doi.org/10.1111/j.1442-9993.1980.tb01243.x

[18] Quality 2 Way Radios. (n.d.). *How far can I talk? UHF vs VHF*. https://quality2wayradios.com/store/radio-range-distance

[19] Stevens, S. (2025). *Urban fire spread modelling: A review of dynamic computational models and potential for application to informal settlement fires*. University of Edinburgh. https://www.pure.ed.ac.uk/ws/portalfiles/portal/486145262/yadav-et-al-2025-atp-regeneration-from-pyruvate-in-the-pure-system.pdf

[20] Tam, A. (2021). *A gentle introduction to particle swarm optimization*. Machine Learning Mastery. https://machinelearningmastery.com/a-gentle-introduction-to-particle-swarm-optimization/

[21] Yang, J. (n.d.). *Forest wildfire monitoring and communication UAV system based on particle swarm optimization*. https://ouci.dntb.gov.ua/en/works/9j5GKjOl/

[22] Yu, S., et al. (2022). Optimal numbers and mix of SSA drones and radio repeater drones based on ant colony algorithm. *Journal of Physics: Conference Series*. https://iopscience.iop.org/article/10.1088/1742-6596/2410/1/012022/pdf

[23] Zirpe, R. (n.d.). *Understanding particle swarm optimization (PSO): From basics to brilliance*. Medium. https://medium.com/@thisisrishi/understanding-particle-swarm-optimization-pso-from-basics-to-brilliance-d0373ad059b6